Electronic Supplementary Material

Ruthenium-doped $Ni(OH)_2$ to enhance the activity of methanol oxidation reaction and promote the efficiency of hydrogen production

Jiajie Lin[a], *Jie Chen* [a,b], *Changhui Tan*[a,b,*], *Yingzhen Zhang*[c,d*], *Yancai Li*[a,b,*]

[a] College of Chemistry, Chemical Engineering and Environment, Minnan Normal University, Zhangzhou 363000, P. R. China

[b] Fujian Province Key Laboratory of Modern Analytical Science and Separation Technology, Minnan Normal University, Zhangzhou 363000, P. R. China

[c] College of Chemical Engineering, Fuzhou University, Fuzhou, 350116, P. R. China

[d] School of Chemistry, Chemical Engineering and Biotechnology, Nanyang Technological University, 637457, Singapore

[*]**Corresponding author: tanchanghui@mnnu.edu.cn; 13338287704@163.com; liyancai@mnnu.edu.cn**

Materials characterization

Transmission Electron Microcopy (TEM) and EDS elemental mapping were observed by JEM 2100F (Japan) at 200 kV. X-ray diffraction (XRD) was carried out on Rigaku Ultima IV diffractometer (Japan) with Cu Kα radiation, scanning speed of 8° min^{-1}, and the 2ϑ range 10° - 80°. Scanning electron microscopy (SEM) was performed on Hitachi S-4800 (Japan) to observe the microstructure and morphology details. under an accelerating voltage of 15.0 kV. X-ray Photoelectron Spectroscopy (XPS) was measured by Escalab 250xi with Al Kα radiation under the condition of 12.5 kV and 250 W (America), the energy of 284.8 eV is used as the basis for correction. High pressure liquid chromatography (HPLC) was recorded on Agilent1200 (America).

Instruments and measurements

The electrochemical experiments were investigated on a CH Instruments (CHI 760 E, Shanghai, China) electrochemical workstation, where, the Ru/$Ni(OH)_2$/NF was shear into 1 * 1 cm and straight employed as the working electrode, the counter electrode: graphite rod, reference electrode: 3 M KCl-saturated Ag/AgCl electrode (CH Instruments, CHI 111), and the electrolyte was 1 M KOH (pH = 14) solution. Potentials were calculated used the reversible hydrogen electrode (RHE) scale (*E vs*. RHE = $E_{Ag/AgCl}$ + 0.059 * pH + 0.197 V).[1] For MOR and HER, electrochemical impedance spectroscopy (EIS) was used at 100000 Hz and 0.01 Hz at the voltage of 0.5 V *vs.* RHE (MOR) and -1.12 V *vs.* RHE (HER), respectively, and an amplitude of 5 mV. Estimated electrochemical double layer capacitance (C_{dl}) was obtained by the cyclic voltammetry (CV) testing in the non-Faraday region between -0.05 V and -0.15 V *vs.* Ag/AgCl with the scan rates from 20 mV s^{-1} to 100 mV s^{-1}. For HER, the CV cycling

stability were swept between 0 ~ -0.8 V *vs.* RHE at a scan rate of 0.1 V·s^{-1}. The linear sweep voltammetry (LSV) were recorded at a scan rate of 5 mV s^{-1}. The *i*-t curves of HER and MOR were tested at potentials of -1.07 V and 0.34 V, respectively. All the electrochemical measurements were proceeded at room temperature of 25° C.

In 1 M KOH with 1 M MeOH at room temperature, the as-synthesized Ru/$Ni(OH)_2$/NF (1×1 cm) was used cathode and anode to investigate the performance of MOR coupled with HER in a single-chamber membrane-less cell, and the electrolyte was 20 mL KOH solution. The polarization curves were collected by linear sweep voltammetry from 1 V to 2 V at a scan rate of 5 mV s^{-1}. The *i*-t measurement at a voltage of 2.1 V, H_2 production was collected by the water displacement method with a 100 mL graduated cylinder.

All electrochemical tests were not *i*R corrected.

Calculation of product (H_2 or formate) yield and faradaic efficiency

The Faraday efficiency (%) of the H_2 and formate can be determined by the following equation:[2, 3]

$$FE = V_{(measured)} / V_{(calculated)}$$

Where *V (measured)* is the experimentally collected gas yield by water displacement method, and *V (calculated)* is the theoretical gas yield, which is calculated as follow:

$$V\ (Calculated) = V_m * [Q / (n * F)]$$

$$FE = (N \times Z \times F / Q) \times 100\%$$

where *N* is the mole of product (H_2 or formate) roduced, V_m is the gas molar volume of 24.5 mol L^{-1} at room temperature and pressure, *Q* is the passed charge, *F* is the Faraday constant (96 485 C mol^{-1}), and *Z* is the number of electrons transferred for a mole of H_2 (*Z* = 2) and

formate (Z = 4) formation.

Energy Consumption Efficiency:[3]

$W = U \times I \times t = U \times Q$, where U is the applied voltage (V), I is the current (A), t is the time (s), and Q is the passed charge (C). When producing the same amount of hydrogen by HER and MOR and HER and OER (consumed the same Q), the required electrical energy of former is $W_1 = U_1 \times Q_1$, while the latter is $W_2 = U_2 \times Q_2$. So $W_1 / W_2 = U_1 / U_2$. The energy consumption saving is equal to $(U_2 - U_1) / U_2 \times 100\%$.

Calculation of ECSA:

ECSA= C_{dl} / C_s * 1, (the specific capacitance (Cs) was taken as 0.060 mF cm^{-2}),[4] the geometric area of the working electrode is 1 cm^2), Current density differences ($\Delta j / 2 = j_a - j_c$) at -0.01 V (*vs.* Ag/AgCl) were plotted against scan rates, the linear slope was used to represent C_{dl}.

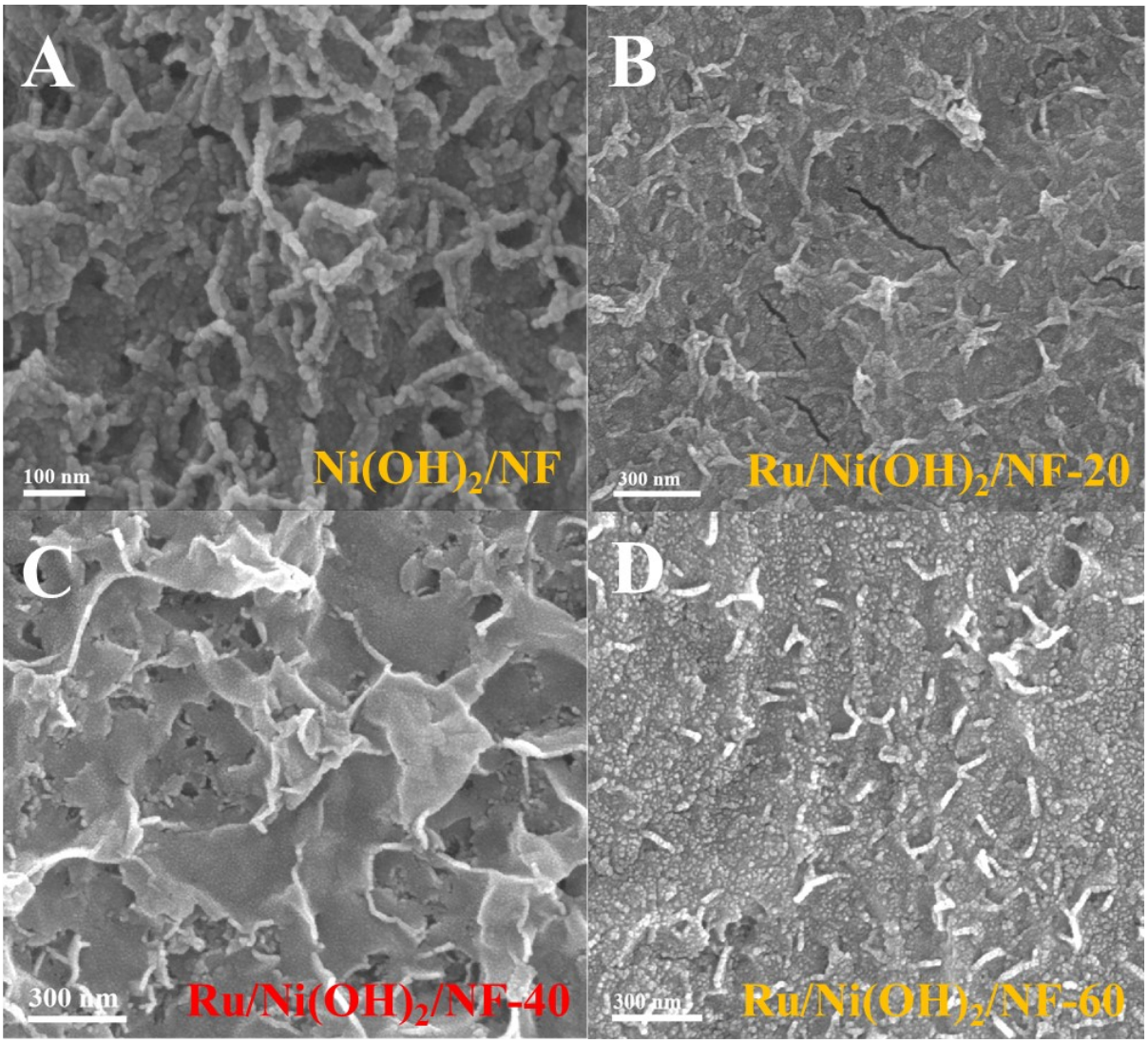

Fig. S1. The SEM image of the $Ni(OH)_2$/NF (A), Ru/$Ni(OH)_2$/NF-20 (B), Ru/$Ni(OH)_2$/NF-40 (C), Ru/$Ni(OH)_2$/NF-60 (D).

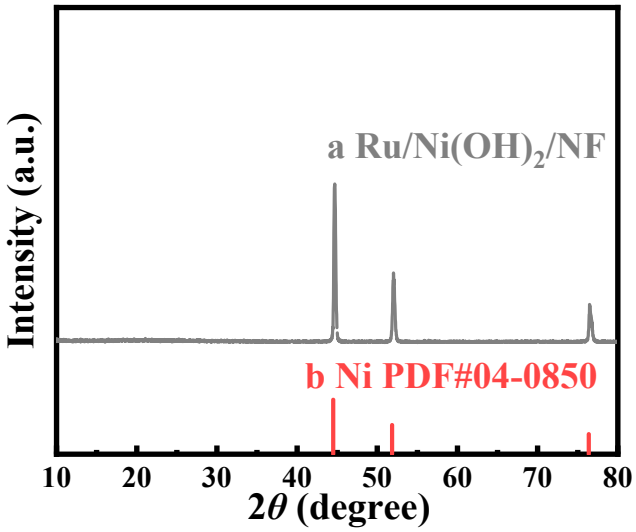

Fig. S2. (A) The XRD patterns of the Ru/Ni(OH)$_2$/NF.

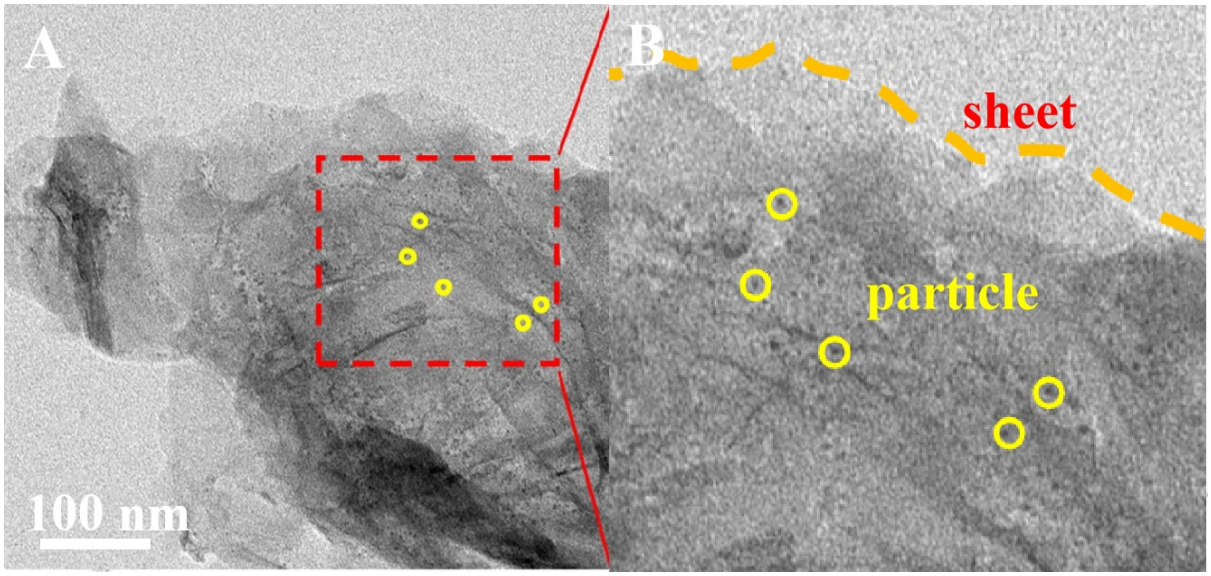

Fig. S3. The HRTEM image of the Ru/Ni(OH)$_2$/NF.

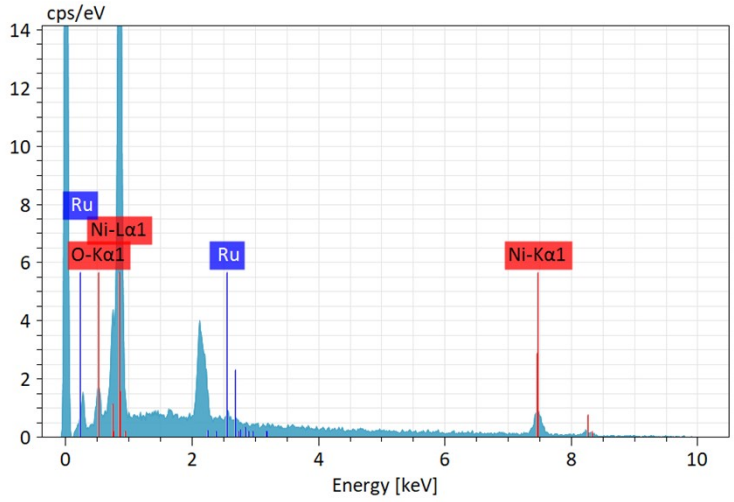

Fig. S4. The EDS image of the Ru/Ni(OH)$_2$/NF

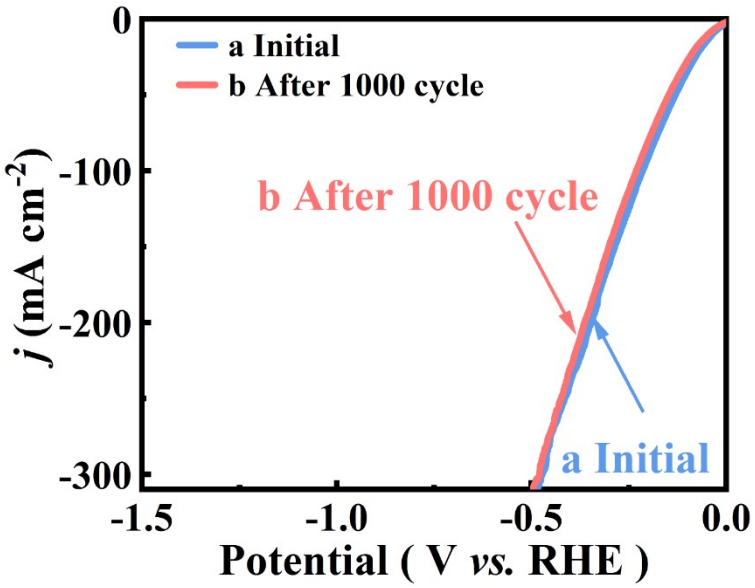

Fig. S5. The LSV curves of the Ru/Ni(OH)$_2$/NF before (a) and after (b) 1000 CV cycles.

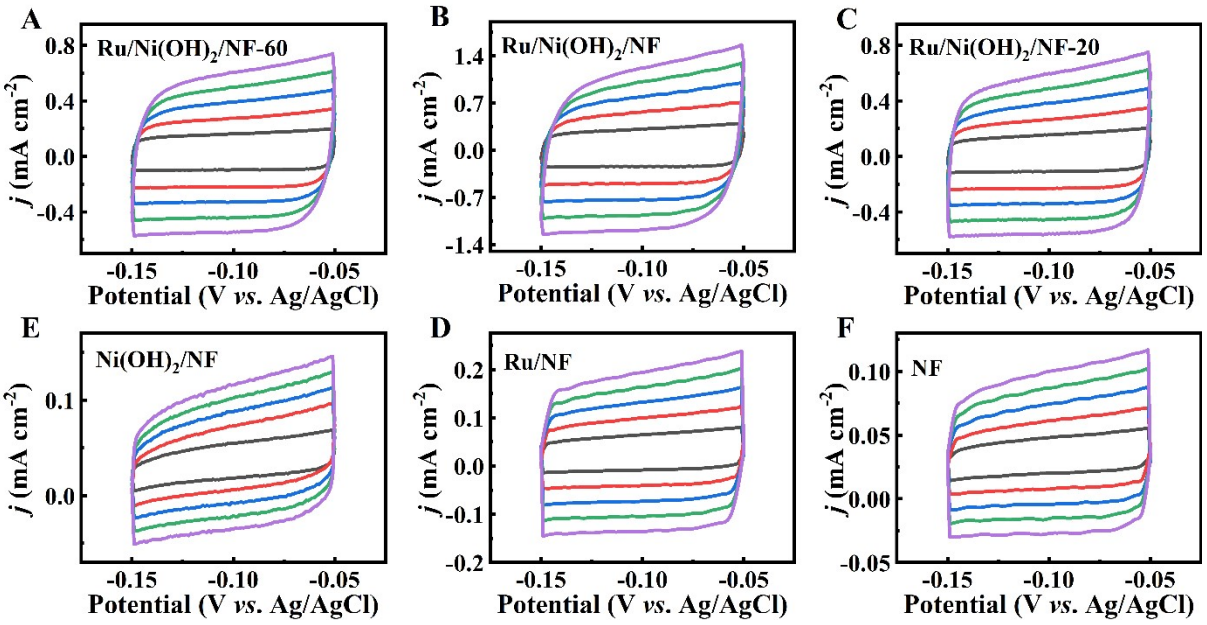

Fig. S6. (A-F) The CV tests of different catalysts, the scanning rates range (20 ~ 100 mV s^{-1}) in 1 M KOH.

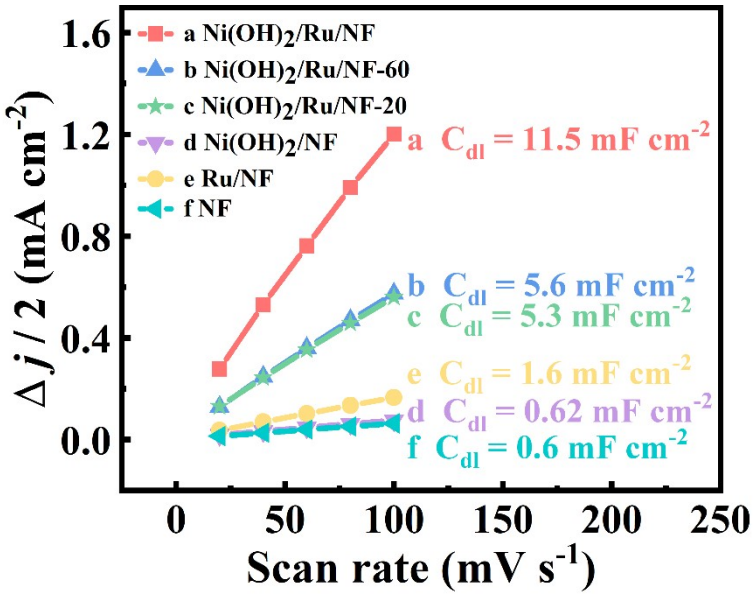

Fig. S7. The corresponding C_{dl} value comparison of the Ru/$Ni(OH)_2$/NF (a), the Ru/$Ni(OH)_2$/NF-60 (b), the Ru/$Ni(OH)_2$/ NF-20(c), the $Ni(OH)_2$/NF (d), the Ru/NF (e) and the NF (f) in 1 M KOH.

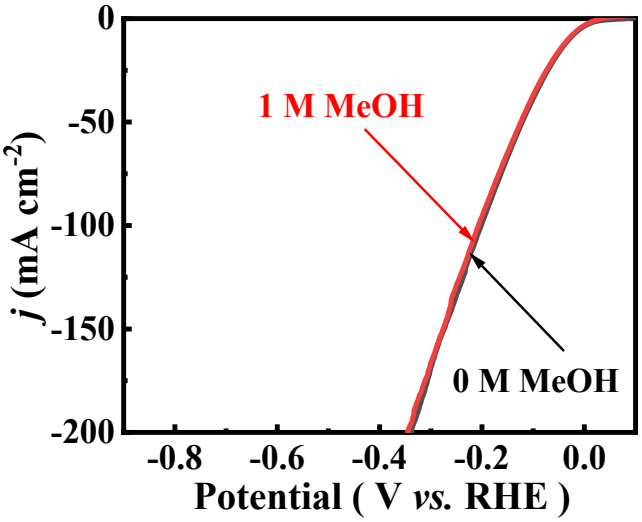

Fig. S8. The LSV curves of the Ru/Ni(OH)$_2$/NF in 1 M KOH with 1 M methanol.

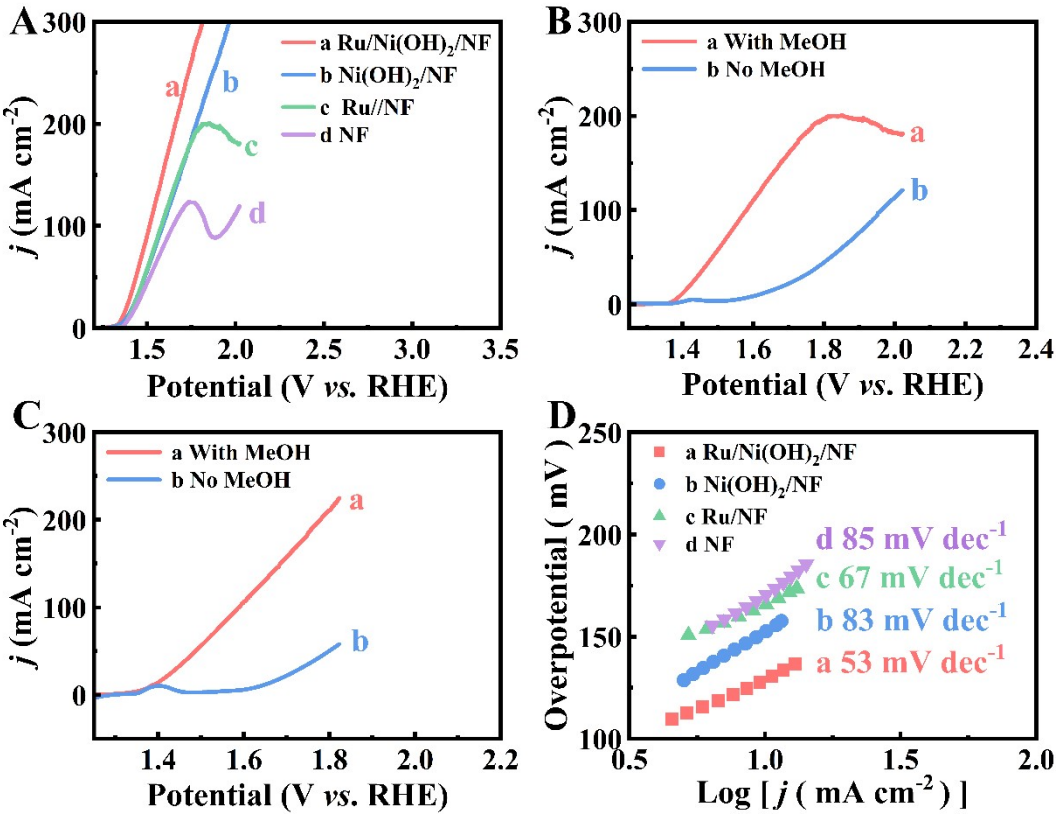

Fig. S9. (A) The LSV curves of the Ru/Ni(OH)$_2$/NF (a), the Ni(OH)$_2$/NF (b), the Ru/NF(c), the NF (d) in 1 M KOH with 1 M MeOH. (B) The LSV curves of the Ru/NF and (C) the Ni(OH)$_2$/NF in 1 M KOH with (a) and without (b) 1 M methanol. (D) Tafel plots of the Ru/Ni(OH)$_2$/NF (a) , the Ni(OH)$_2$/NF (b), the Ru/NF(c), the NF (d) in 1 M KOH with 1 M MeOH.

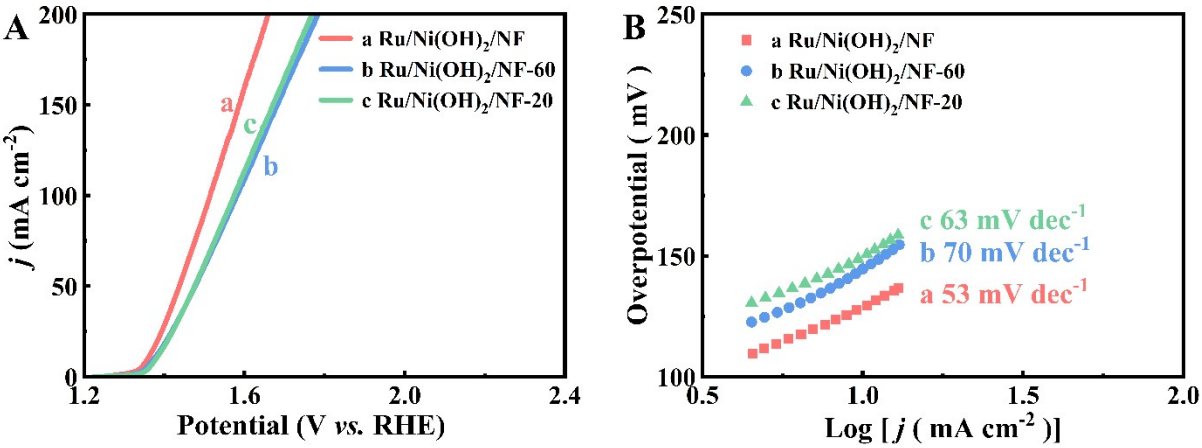

Fig. S10. (A) The LSV curves and (B) Tafel plots of the Ru/Ni(OH)$_2$/N (a), the Ru/Ni(OH)$_2$/NF-60 (b), the Ru/Ni(OH)$_2$/NF-20 (c) in 1 M KOH with 1 M MeOH.

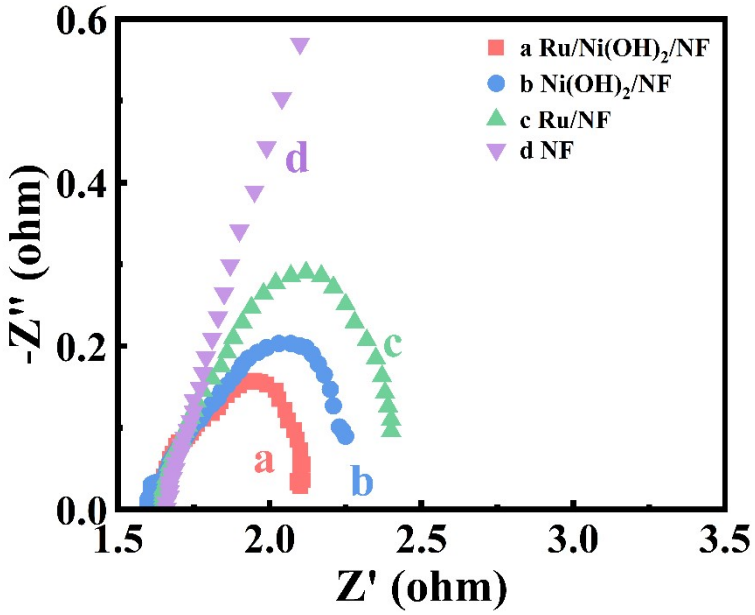

Fig. S11. The electrochemical impedance spectroscopy (EIS) analyses of the catalysts for methanol oxidation. Nyquist plots of the Ru/Ni(OH)$_2$/NF (a), the Ni(OH)$_2$/NF (b), the Ru/NF (c) and the NF (d) for methanol electro-oxidation process in 1 M KOH with 1 M methanol.

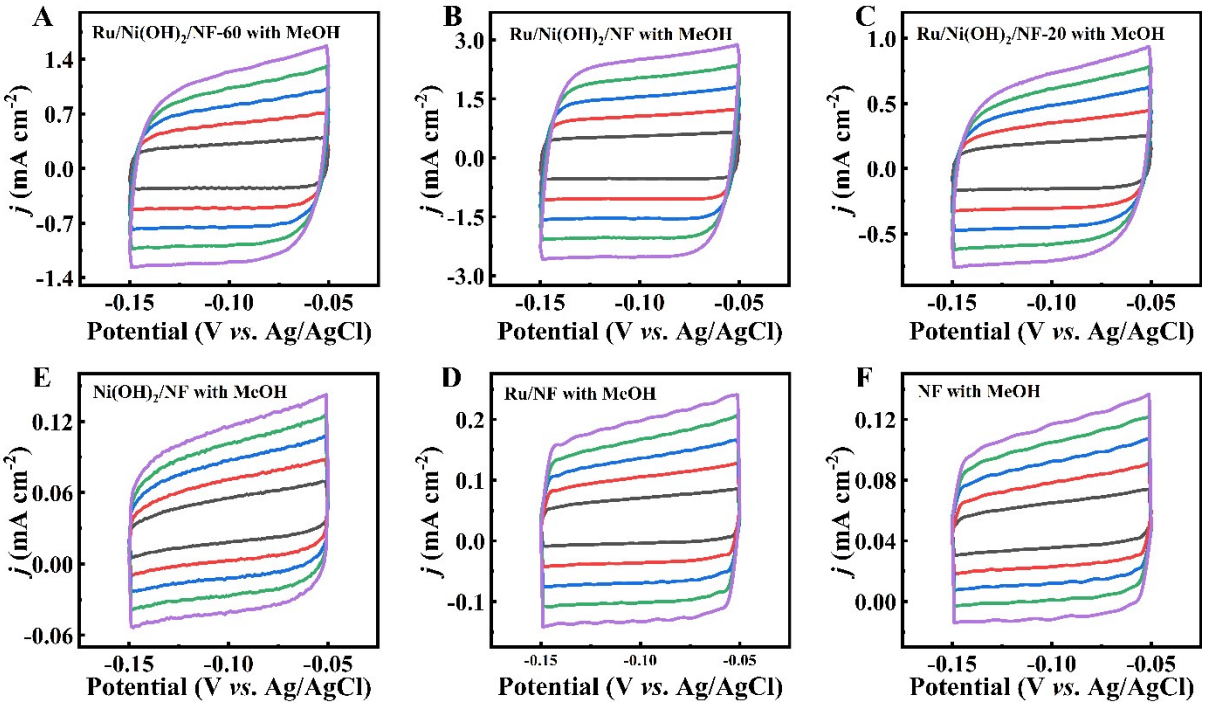

Fig. S12. (A-F) The CV tests of different catalysts, the scanning rates range (20 mV s^{-1} ~ 100 mV s^{-1}) in 1 M KOH with 1 M methanol.

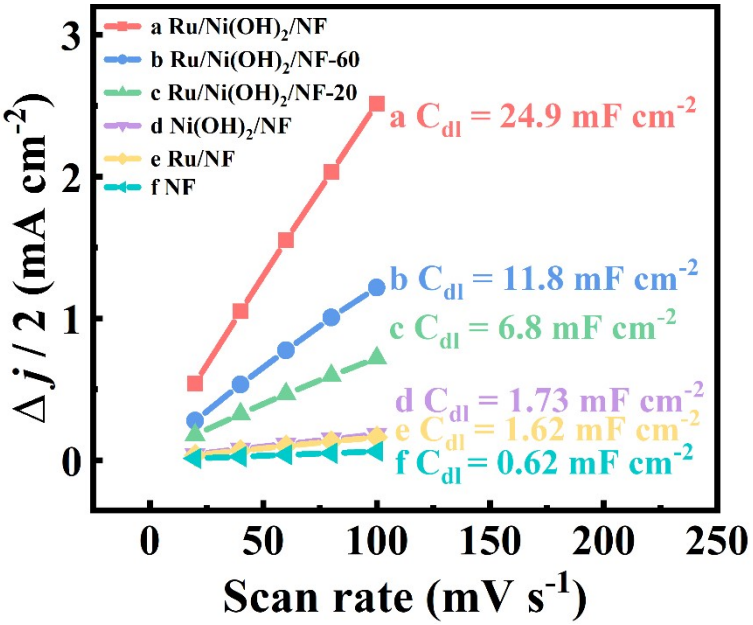

Fig. S13. The corresponding C_{dl} value comparison of the Ru/$Ni(OH)_2$/NF (a), the Ru/$Ni(OH)_2$/NF-60 (b), the Ru/$Ni(OH)_2$/NF-20 (c), the $Ni(OH)_2$/NF (d), the Ru/NF (e), and the NF (f) in 1 M KOH with 1 M MeOH.

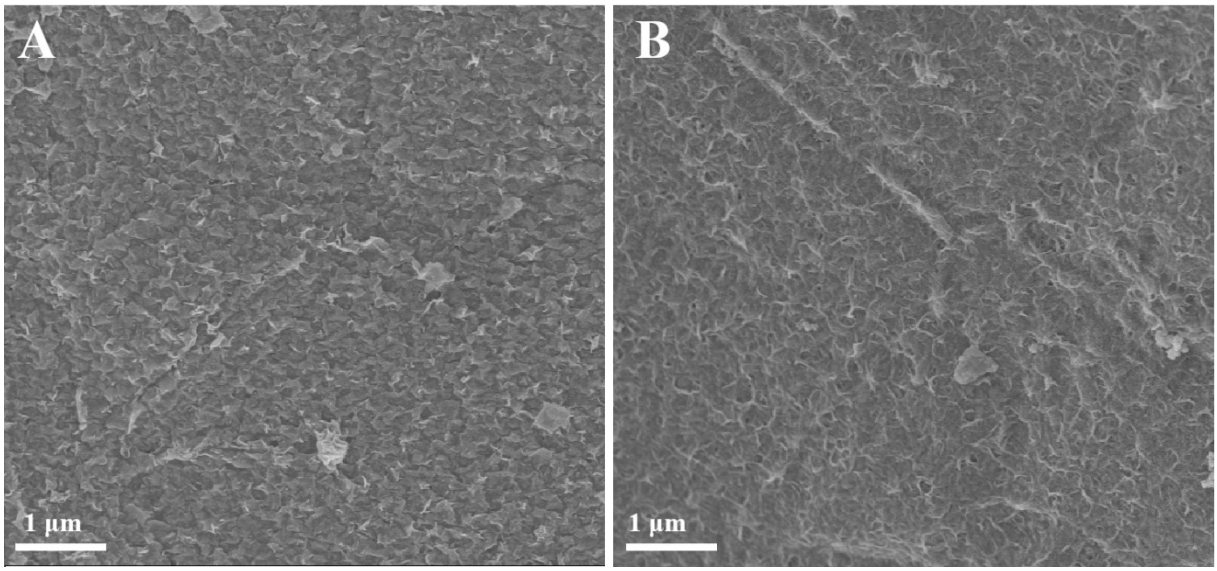

Fig. S14 The SEM images of the Ru/$Ni(OH)_2$/NF after 1000 cycles of CV cycle stability of HER (A) and MOR test (B).

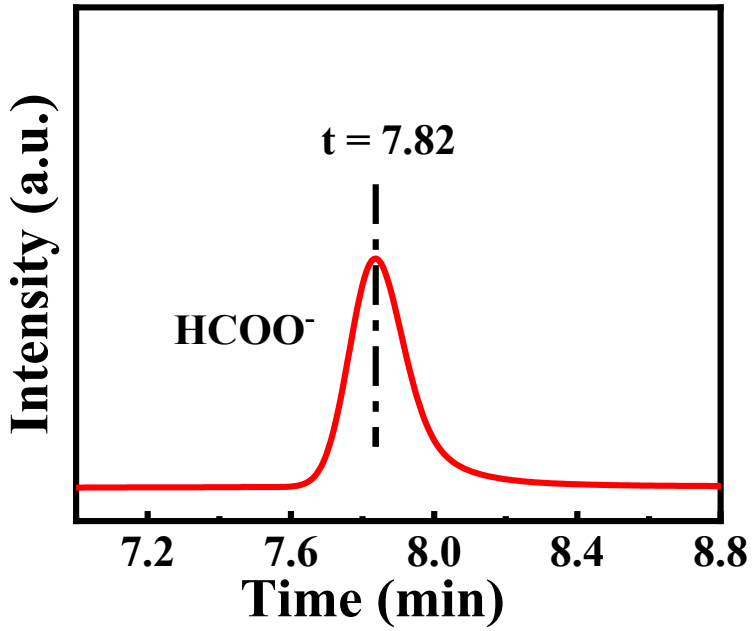

Fig. S15. Formate standard materials were tested on the HPLC.

Table S1. Comparison of the HER performances of various catalysts in 1 M KOH.

Catalysts	iR compensation	Electrode	Overpotentia (mV) @ 10 mA/cm^2	Ref.
Ru/Ni(OH)$_2$/NF	**0%**	**NF**	**42**	**This work**
MoP-Ru$_2$P/NPC	95%	GCE	47	[5]
Ru/Ni(OH)$_2$/TM-0.2	95%	Ti mesh	135	[6]
(Ru-Co)O$_x$/CC	95%	CC	44.1	[7]
CoSA-NC@Ru	95%	CC	14	[8]
Ru/Ni(OH)$_2$/NF	95%	NF	25	[9]
Ru/Ni(OH)$_2$	80%	CP	31	[10]
R-NiRu/NF	95%	NF	16	[11]
Ru-NC-700	85%	GCE	47	[12]

Table S2. Representative electrochemical reformingc of the MOR.

catalysts	Electrolyte	Main anode product	Cell voltage at 10 mA cm^{-2} (V)	Ref.
$Ru/Ni(OH)_2/NF$	**1 M KOH + 1 M methanol**	**formate**	**1.36**	**this work**
NiMoO/NF	1 M KOH + 0.5 M Urea	N_2, CO_2	1.37	[13]
CoCu-UMOF Ns	1 M KOH + 3 M methanol	formate	1.365	[14]
Co_3O_4 NSs/CP	1 M KOH + 1 M Ethanol	Ethyl acetate	1.445	[15]
Co_3O_4 NWs/CC	1 M KOH + 40 mg L^{-1} triclosan	Phenol	1.54	[16]
Ni-MOF	1 M KOH + 0.33 M Urea	N_2, CO_2	1.36	[17]
NF-Pt/C	1 M KOH + 0.5 M Urea	N_2, CO_2	1.48	[18]
Co@NPC-800	1 M KOH + 0.1 M glucose	formate	1.46	[19]

Table S3. Comparison of the chemical-assisted hydrogen evolution reaction performance.

Bifunctional catalysts	Electrolyte	Main anode product	Cell voltage at 10 mA cm^{-2} (V)	Ref.
Ru/Ni(OH)$_2$/NF	**1 M KOH + 1 M methanol**	**formate**	**1.45**	**this work**
Pd/Ni(OH)$_2$@C/NF	1 M KOH + 1 M ethanol	-	1.49	[20]
Co-Rh$_2$	1 M KOH + 1 M methanol	formate	1.55	[21]
Ni(OH)$_2$/NF	1 M KOH + 0.5 M methanol	formate	1.52	[22]
MnO_2/$MnCo_2O_4$/Ni	1 M KOH + 0.5 M Urea	N_2, CO_2	1.58	[23]
$Ni_{0.33}Co_{0.67}(OH)_2$/NF	1 M KOH + 0.5 M methanol	formate	1.50	[24]
Os-Ni_xP/N-C/NF	1 M KOH + 1 M methanol.	formate	1.43	[25]
NiAl-LDH-NS_s	1 M KOH + 1 M ethanol	formate	1.72	[26]
Co-S-P/CC	1 M KOH + 1 M ethanol	acetic acid	1.63	[27]

References

1. Z. Y. Duan, T. L. Ren, Q. Q. Mao, H. J. Yu, K. Deng, Y. Xu, Z. Q. Wang, L. Wang and H. J. Wang, *Journal of Materials Chemistry A*, 2022, **10**, 18126-18131.
2. Y. Guo, X. Yang, X. Liu, X. Tong and N. Yang, *Advanced Functional Materials*, 2023, **33**, 2209134.
3. K. Xiang, D. Wu, X. H. Deng, M. Li, S. Y. Chen, P. P. Hao, X. F. Guo, J. L. Luo and X. Z. Fu, *Advanced Functional Materials,* 2020, **30**, 1909610.
4. Z. S. Lin, S. L. Liu, Y. G. Liu, Z. Liu, S. D. Zhang, X. F. Zhang, Y. Tian and Z. H. Tang, *Journal of Power Sources*, 2021, **514**, 230600.
5. Y. X. Gao, Z. Chen, Y. Zhao, W. L. Yu, X. L. Jiang, M. S. He, Z. J. Li, T. Y. Ma, Z. X. Wu and L. Wang, *Applied Catalysis B: Environmental*, 2022, **303**, 120879.
6. Y. J. Wang, J. K. Wang, T. P. Xie, Q. Y. Zhu, D. Zeng, R. Li, X. D. Zhang and S. L. Liu, *Applied Surface Science*, 2019, **485**, 506-512.
7. C. Wang and L. Qi, *Angew Chem Int Ed Engl*, 2020, **59**, 17219-17224.
8. Y. B. Jeong and S. Hoon Ahn, *Chemical Engineering Journal*, 2022, **437**, 135322.
9. Q. Q. Chen, X. Yang, C. C. Hou, K. Li and Y. Chen, *Journal of Materials Chemistry A*, 2019, **7**, 11062-11068.
10. W. D. Ao, C. G. Cheng, H. J. Ren, Z. S. Fan, P. Q. Yin, Q. Qin, Z. N. Chen and L. Dai, *ACS Applied Materials & Interfaces*, 2022, **14**, 45042-45050.
11. X. Y. Chen, J. W. Wan, J. Wang, Q. H. Zhang, L. Gu, L. R. Zheng, N. Wang and R. B. Yu, *Advanced Materials*, 2021, **33**, 2104764.

12. B. Lu, L. Guo, F. Wu, Y. Peng, J. E. Lu, T. J. Smart, N. Wang, Y. Z. Finfrock, D. Morris, P. Zhang, N. Li, P. Gao, Y. Ping and S. Chen, *Nature Communications*, 2019, **10**, 631.

13. F. d. C. Romeiro, A. S. Martins, J. A. L. Perini, B. C. e. Silva, M. V. B. Zanoni and M. O. Orlandi, *Journal of Materials Science*, 2023, **58**, 3508-3519.

14. Y. X. Sun, A. J. Huang, Z. J. Li, Y. Q. Fu and Z. G. Wang, *Electrocatalysis*, 2022, **13**, 494-501.

15. P. J. Wang, Y. T. Yan, P. C. Wang, Z. Y. Ye, X. H. Zheng and W. Cai, *Chemical Engineering Journal*, 2023, **455**, 140856.

16. Y. Song, J. Cheng, J. Liu, Q. Ye, X. Gao, J. Lu and Y. Cheng, *Applied Catalysis B: Environmental*, 2021, **298**, 120488.

17. C. Li, S. H. Kim, H. Y. Lim, Q. Sun, Y. Jiang, H. J. Noh, S. J. Kim, J. Baek, S. K. Kwak and J. B. Baek, *Advanced Materials*, 2023, **35**, 01369.

18. A. Meena, M. Ha, S. S. Chandrasekaran, S. Sultan, P. Thangavel, A. M. Harzandi, B. Singh, J. N. Tiwari and K. S. Kim, *Journal of Materials Chemistry A*, 2019, **7**, 15794-15800.

19. Q. Hong, Y. M. Wang, R. R. Wang, Z. L. Chen, H. Y. Yang, K. Yu, Y. Liu, H. Huang, Z. H. Kang and P. W. Menezes, *Small*, 2023, **19**, 2206723.

20. C. Li, H. Wen, P. P. Tang, X. P. Wen, L. S. Wu, H. B. Dai and P. Wang, *ACS Applied Energy Materials*, 2018, **1**, 6040-6046.

21. Y. Guo, X. B. Yang, X. C. Liu, X. L. Tong and N. J. Yang, *Advanced Functional Materials*, 2023, **33**, 2209134.

22. J. Hao, J. W. Liu, D. Wu, M. X. Chen, Y. Liang, Q. Wang, L. Wang, X. Z. Fu and J. L. Luo, *Applied Catalysis B: Environmental*, 2021, **281**, 119510.

23. C. L. Xiao, S. N. Li, X. Y. Zhang and D. R. MacFarlane, *Journal of Materials Chemistry A*, 2017, **5**, 7825-7832.

24. M. Li, X. Deng, K. Xiang, Y. Liang, B. Zhao, J. Hao, J. L. Luo and X. Z. Fu, *ChemSusChem*, 2020, **13**, 914-921.

25. Z. Y. Duan, T. L. Ren, Q. Q. Mao, H. J. Yu, K. Deng, Y. Xu, Z. Q. Wang, L. Wang and H. J. Wang, *Journal of Materials Chemistry A*, 2022, **10**, 18126-18131.

26. L. Xu, Z. Wang, X. Chen, Z. K. Qu, F. Li and W. S. Yang, *Electrochimica Acta*, 2018, **260**, 898-904.

27. S. Sheng, K. Ye, L. N. Sha, K. Zhu, Y. Y. Gao, J. Yan, G. L. Wang and D. X. Cao, *Inorganic Chemistry Frontiers*, 2020, **7**, 4498-4506.